Acta Crystallographica Section F
Structural Biology and Crystallization Communications
ISSN 1744-3091

Purification, crystallization and preliminary X-ray analysis of the ligand-binding domain of human lectin-like oxidized low-density lipoprotein receptor 1 (LOX-1)

Tomoko Ishigaki,[a] Izuru Ohki,[a] Takuji Oyama,[a] Sachiko Machida,[b] Kousuke Morikawa[a] and Shin-ichi Tate[a]*

[a]Department of Structural Biology, Biomolecular Engineering Research Institute (BERI), 6-2-3 Furuedai, Suita, Osaka 565-0874, Japan, and [b]National Food Research Institute, Tsukuba, Ibaraki 305-8642, Japan

Correspondence e-mail: tate@beri.or.jp

Received 16 February 2005
Accepted 18 April 2005
Online 28 April 2005

Two different fragments of the ligand-binding domain of LOX-1, the major receptor for oxidized low-density lipoprotein (LDL) on endothelial cells, have been crystallized in different forms. One crystal form contains the disulfide-linked dimer, which is the form of the molecule present on the cell surface; the other contains a monomeric form of the receptor that lacks the cysteine residue necessary to form disulfide-linked homodimers. The crystal of the monomeric ligand-binding domain belongs to space group $P2_12_12_1$, with unit-cell parameters $a = 56.79$, $b = 67.57$, $c = 79.02$ Å. The crystal of the dimeric form belongs to space group $C2$, with unit-cell parameters $a = 70.86$, $b = 49.56$, $c = 76.73$ Å, $\beta = 98.59°$. Data for the dimeric form of the LOX-1 ligand-binding domain have been collected to 2.4 Å. For the monomeric form of the ligand-binding domain, native, heavy-atom derivative and SeMet-derivative crystals have been obtained; their diffraction data have been measured to 3.0, 2.4 and 1.8 Å resolution, respectively.

1. Introduction

The lectin-like oxidized low-density lipoprotein (LDL) receptor, LOX-1, was identified as the major receptor for oxidized LDL (OxLDL) in endothelial cells of large arteries (Chen *et al.*, 2002; Sawamura *et al.*, 1997). OxLDL binding to LOX-1 causes endothelial dysfunction, subsequent induction of adhesion molecules and endothelial apoptosis (Cominacini *et al.*, 2000, 2001; Li & Mehta, 2000*a*,*b*). LOX-1 is also present in atheroma-derived cells and accumulates in atherosclerosis lesions (Chen *et al.*, 2000; Kataoka *et al.*, 1999). OxLDL binding to LOX-1 in vascular smooth-muscle cells can induce their apoptosis (Kataoka *et al.*, 2001), which suggests that LOX-1 is involved in the destabilization and rupture of atherosclerotic plaques. High concentrations of the lipoprotein LOX-1 ligand, together with the higher expression of LOX-1, in atherosclerotic lesions provide a molecular basis for the link between OxLDL and endothelial cellular dysfunction and injury (Kita, 1999; Kita *et al.*, 2001). Accumulating data suggest that inhibitors of LOX-1 binding to OxLDL may provide a therapeutically important approach for vascular diseases, particularly atherosclerosis (Chen *et al.*, 2002), which has motivated us to solve the LOX-1 structure in order to elucidate the details of its ligand-recognition mechanism.

LOX-1 is a membrane protein with a type II orientation consisting of four domains: a short cytoplasmic domain, a single transmembrane domain, a stalk region called the 'NECK' and a C-type lectin-like domain (CTLD) that functions as the ligand-binding domain (Chen *et al.*, 2001). A comparison of recent structures of CTLDs has revealed diversity in the modular fold (Drickamer, 1999). Sequence analysis suggests that the divergent evolution of a precursor to the CTLDs has resulted in several groups of domains with distinct functions (Drickamer, 1999). The CTLD fold is classified into seven groups with different functions as follows: C-type lectins, which bind to carbohydrates, coagulation factor-binding proteins, the IgE Fc receptor, type II antifreeze proteins, phopholipase receptors, natural killer cell (NK-cell) receptors and the oxidized LDL receptor (Drickamer, 1999). Representative structures of some of these groups of the CTLD have been solved, including C-type lectins (Weis *et al.*, 1991, 1992; Weis & Drickamer, 1994) and NK-cell receptors (Natarajan *et al.*, 2002), but no CTLD structure in the OxLDL receptor

© 2005 International Union of Crystallography
All rights reserved

group has been solved so far. Although the CTLD proteins share a global architecture, significant diversity in the modular fold, particularly in the ligand-binding long-loop region (LLR), is apparent among the available CTLD structures (Drickamer, 1999).

The structure of LOX-1 thus provides the first representative structure in the OxLDL receptor group of the CTLD family of proteins. Here, we describe the purification procedure used to obtain the actively refolded LOX-1 protein from insoluble inclusion bodies expressed in bacterial cells, as well as the crystallization of the LOX-1 CTLD.

2. Materials and methods

2.1. Protein expression, refolding from inclusion bodies and purification

Human LOX-1 cDNA was cloned from human aortic endothelial cells (HAEC; Shi *et al.*, 2001). Two variants of the extracellular domain fragment of human LOX-1 were cloned into the expression vector pET28a (Novagen): a fragment containing only the CTLD (residues 143–273) and the CTLD plus the 14-residue NECK domain (CTLD-NECK14; 129–273). The proteins were expressed with a His_6 tag at their N-termini.

Escherichia coli strain BL21(DE3) transformed with plasmids expressing the LOX-1 proteins was grown in synthetic minimal M9 medium with 50 µg ml^{-1} kanamycin at 310 K until it reached an optical density of 0.5 at 660 nm. Protein expression was induced by adding 1 m*M* isopropyl-1-thio-β-D-galactopyranoside (IPTG). After induction, culture was continued for 6 h at 310 K. The cells were harvested by centrifugation and disrupted by sonication in buffer solution comprising 50 m*M* Tris–HCl pH 8.0, 400 m*M* NaCl and 0.1%(*v*/*v*) Triton X-100. The precipitant collected by centrifugation from the cell lysate was dissolved in a solution containing 6 *M* guanidium hydrochloride, 50 m*M* Tris–HCl pH 8.0 and 50 m*M* dithiothreitol (DTT). After dissolving the precipitant, the solution was kept at room temperature for 4 h.

Protein refolding in this work basically followed the procedure used in preceding work (Li *et al.*, 1998; Natarajan *et al.*, 2000), optimizing the experimental conditions for LOX-1. The solubilized protein solution from the precipitant was titrated dropwise into refolding buffer solution comprising 50 m*M* Tris–HCl pH 8.5, 0.4 *M* L-arginine and a mixture of 5 m*M* reduced/0.5 m*M* oxidized glutathione (GSH/GSSG). The diluted protein solution was dialyzed against a buffer solution of 25 m*M* Tris–HCl pH 7.5 and 50 m*M* NaCl and then applied onto a HisTrap HP Ni-affinity column (Amersham Pharmacia Biotech). The protein that eluted from the Ni-affinity column was subjected to size-exclusion chromatography (HiLoad Superdex 75 26/60, Amersham Pharmacia Biotech) after the N-terminal His_6 tag had been cleaved by thrombin. For the LOX-1 CTLD fragment, a buffer solution comprising 10 m*M* Tris–HCl pH 7.5 and 50 m*M* NaCl was used for elution; for the CTLD-NECK14 fragment, the salt concentration was increased to 400 m*M* NaCl.

Fractions containing the purified protein were concentrated with Centriplus10 and Centricon10 (Amicon). The final protein concentration was determined by UV-absorbance spectroscopy. Both types of refolded LOX-1 fragment showed the same binding specificity and affinity for OxLDL, as determined by surface plasmon resonance using CM-sensors doped with the purified LOX-1 fragments (Biacore 2000, Pharmacia).

Dimer formation of the CTLD-NECK14 fragment was confirmed by SDS–PAGE under reducing and non-reducing conditions (Fig. 1*a*). The LOX-1 CTLD-NECK14 fragment migrates at the expected molecular weight for a monomer under reducing conditions, but migrates as a dimer in the absence of β-mercaptoethanol. In contrast, the mobility of the LOX-1 CTLD fragment was similar under reducing and non-reducing conditions. The slight shift in mobility that is observed for LOX-1 CTLD under reducing conditions can be ascribed to the structural changes associated with cleaving the three disulfide bonds in the CTLD.

Each LOX-1 fragment was further analyzed by analytical ultracentrifugation experiments. The experiments were carried out at 293 K using a Beckman Optima XL-1 instrument. LOX-1 CTLD and CTLD-NECK14 fragments were dialyzed against 10 m*M* Tris–HCl buffer pH 7.5 containing 50 m*M* NaCl (for CTLD) or 400 m*M* NaCl (for CTLD-NECK14) and each fragment was concentrated to 0.1 mg ml^{-1}. Equilibrium distributions for the LOX-1 CTLD and

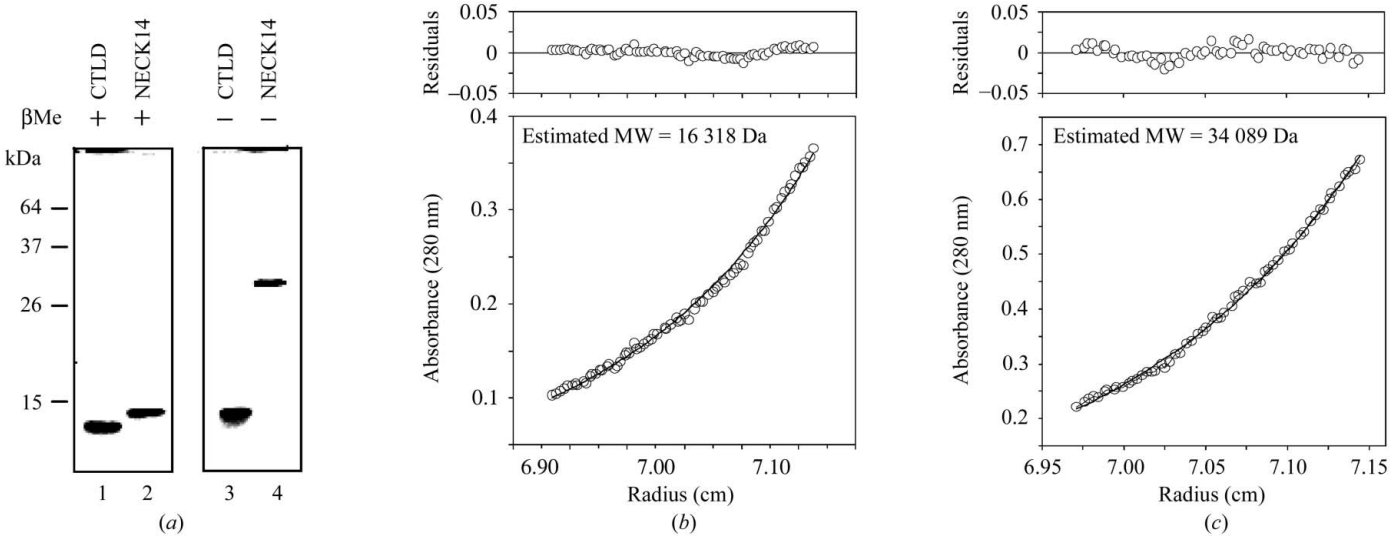

Figure 1
(*a*) SDS–PAGE of the purified LOX-1 fragments. CTLD and NECK14 denote LOX-1 CTLD (residues 142–273) and CTLD-NECK14 (residues 129–273), respectively. The results for the samples treated with β-mercaptoethanol (left panel, labelled βMe +) and those without reduction (right panel, βMe −) are compared. (*b*) and (*c*) show the results of the analytical ultracentrifugation for the LOX-1 fragments LOX-1 CTLD (*b*) and CTLD-NECK14 (*c*). Curve fitting to the experimental data using a single-component model and the residual of the observed data from the fitted model curve are shown along with the estimated molecular weight.

Table 1
Data-collection statistics for LOX-1 CTLD monomer and CTLD-NECK14 homodimer.

Values in parentheses are for the last shell.

	CTLD monomer			
	Native	SeMet derivative	Heavy-atom derivative with PtIPt	CTLD-NECK14 dimer
Crystal data				
Crystallization pH	3.6–3.8	4.0–4.2	3.0–3.8	7.5
Space group	$P2_12_12_1$	$P2_12_12_1$	$P4_12_12$	$C2$
Unit-cell parameters				
a (Å)	56.79	62.76	64.41	70.86
b (Å)	67.57	69.08	64.41	49.54
c (Å)	79.02	79.33	79.80	76.73
β (°)				98.59
Data collection				
Wavelength (Å)	1.5418	1.0000	1.5418	1.0000
Resolution (Å)	50.0–3.0 (3.11–3.00)	50.0–1.78 (1.84–1.78)	30.0–2.4 (2.49–2.40)	37.9–2.40 (2.49–2.40)
Unique reflections	6438 (593)	33424 (3277)	6978 (672)	10449 (1009)
Completeness (%)	99.1 (95.2)	99.6 (99.7)	99.4 (98.5)	99.3 (99.3)
R_{merge}† (%)	10.0 (21.8)	5.3 (39.5)	6.3 (38.2)	8.1 (36.4)
Redundancy	3.8 (3.8)	3.6 (3.2)	7.4 (7.4)	3.7 (3.7)
Mosaicity	1.2	0.3	0.4	1.0

† $R_{merge} = \sum |I_{obs} - \langle I \rangle| / \sum I_{obs}$.

CTLD-NECK14 fragments were analyzed after 36 h centrifugation at 8000 and 15 000 rev min^{-1}, respectively, using a Beckman An-50Ti rotor with double-sector centerpiece. For the molecular-weight calculation, the data were fitted to an ideal single-component model. The estimated molecular weight for the LOX-1 CTLD was close to the expected value from its amino-acid composition, 14 952 Da, showing that it behaves as monomer in solution (Fig. 1*b*). On the other hand, the apparent molecular weight for the LOX-1 CTLD-NECK14 was estimated to 34 089 Da, which corresponds to the molecular weight of its dimeric form; the molecular weight of the monomeric LOX-1 CTLD-NECK14 from amino-acid composition is 16 481 Da (Fig. 1*c*).

2.2. Crystallization

Crystals of the LOX-1 CTLD fragment grew from an equal volume mixture of protein solution (8.0 mg ml^{-1} protein, 10 m*M* Tris–HCl pH 7.5, 50 m*M* NaCl) and precipitant solution (100 m*M* citrate pH 3.6) at 293 K. Crystals of the platinum derivative of the LOX-1 CTLD fragment were prepared by soaking the crystals overnight at 293 K in the above precipitant solution plus 1 m*M* PtIPt [di-μ-iodobis(ethylenediamine) diplatinum (II) nitrate]. Crystals of the SeMet derivative of the LOX-1 CTLD were obtained by slightly modifying the above conditions; in brief, protein solution (7.6 mg ml^{-1} protein, 10 m*M* Tris–HCl pH 7.5, 50 m*M* NaCl) was mixed with precipitant solution (100 m*M* citrate pH 4.0–4.2) containing 20 m*M* zinc acetate.

The NECK14-CTLD fragment was crystallized at physiological pH from a solution made from an equivolume mixture of protein solution (4.6 mg ml^{-1} protein, 10 m*M* Tris–HCl pH 7.5, 400 m*M* NaCl) and precipitant solution (100 m*M* HEPES buffer pH 7.5, 20% PEG 10K; Crystal Screen 2 No. 38, Hampton Research) at 277 K.

2.3. Data collection

For the SeMet derivative of the LOX-1 CTLD, diffraction data were collected at beamline BL40-B2 at SPring-8, Harima, Japan. The diffraction data were recorded on an ADSC Quantum-4 CCD scanner and processed using the *HKL*2000 software package (Otwinowski & Minor, 1997). Data for the heavy-atom (PtIPt) derivative and the native were collected on an in-house X-ray diffractometer. Data for the CTLD-NECK14 fragment were collected at beamline BL-6B at the Photon Factory (PF) of the National Laboratory for High Energy Physics, Tsukuba, Japan. The diffraction data were recorded on a Rigaku R-AXIS IV^{++} imaging-plate detector and processed using *CrystalClear* (Molecular Structure Corporation; Pflugrath, 1999). Cryocooling required that the crystals were immersed in cryoprotectant, comprising reservoir solution plus 20%(*v*/*v*) ethylene glycol, for several seconds immediately prior to their exposure to a stream of N_2 gas at 100 K for data collection. Data-collection and scaling statistics are given in Table 1.

2.4. Crystallization and X-ray crystallographic analysis

Rod-shaped native crystals of the LOX-1 CTLD appeared after 4 d and grew to dimensions of about 0.4 × 0.05 × 0.05 mm within a week. For the SeMet derivative of the LOX-1 CTLD fragment, the crystal volume was increase by adding zinc or calcium. Crystals prepared from the zinc-containing solution including ethylene glycol as a cryoprotectant gave better X-ray diffraction data at 100 K than those prepared without zinc or other divalent cations. Crystals for the heavy-atom derivative of LOX-1 CTLD fragment with PtIPt gave better diffraction (to 2.6 Å) than native crystals.

Crystals of the LOX-1 CTLD-NECK14 fragment, which contains an interchain disulfide bond to retain the homodimeric form, appeared eight months after preparation at 277 K. A piece of crystal was picked up from a cluster for diffraction which had a size of about 0.2 × 0.05 × 0.05 mm. Data were collected from this native crystal to 2.4 Å.

3. Discussion

For detailed elucidation of the function of LOX-1 the structure of the homodimer is essential, because human LOX-1 belongs to group V of the CTLD family of proteins, which exist on the cell surface as disulfide-linked homodimers or heterodimers (Drickamer, 1999; Drickamer & Dodd, 1999). While crystallographic dimers have been observed for various CTLD proteins, many of these dimers have been observed in the absence of the NECK domain. The physiological relevance of such dimer structures is unclear, since examples are known where the same protein adopts different oligomerization modes in the presence and absence of the NECK domain (Drickamer, 1999; Sheriff *et al.*, 1994; Weis *et al.*, 1991; Weis & Drickamer, 1994). Because the CTLD domain of LOX-1 alone does not form a

dimer in solution (Fig. 1*b*), the structure of the covalent LOX-1 dimer will be essential for understanding the ligand-recognition modes of the protein.

The present LOX-1 CTLD disulfide-linked dimer was crystallized serendipitously after a long stay in the crystallization chamber. During the crystallization, part of the N-terminal NECK region was cleaved by a small amount of proteases contained in the sample solution. N-terminal sequence analysis of the crystallized fragment has shown that nine N-terminal residues were removed from the original CTLD-NECK14 fragment. The cysteine residue that forms the inter-chain disulfide bond was retained in the fragment. The removal of the highly flexible N-terminal part of the CTLD-NECK14 fragment must have helped the crystallization of the LOX-1 disulfide-linked dimer. The LOX-1 CTLD structure will be determined with MAD techniques using the SeMet-derivative. Subsequently, the disulfide-linked dimeric structure of LOX-1 CTLD-NECK14 will be determined by molecular replacement using the monomeric LOX-1 CTLD structure.

We thank Drs Noriyoshi Sakabe and Kazutaka Demura for use of the facilities at the Photon Factory and Dr Nobutaka Shimizu for use of the facilities at SPring-8. This work was supported by New Energy and Industrial Technology Development Organization (NEDO).

References

Chen, M., Kakutani, M., Minami, M., Kataoka, H., Kume, N., Narumiya, S., Kita, T., Masaki, T. & Sawamura, T. (2000). *Arterioscler. Thromb. Vasc. Biol.* **20**, 1107–1115.
Chen, M., Masaki, T. & Sawamura, T. (2002). *Pharmacol. Ther.* **95**, 89–100.
Chen, M., Narumiya, S., Masaki, T. & Sawamura, T. (2001). *Biochem. J.* **355**, 289–296.
Cominacini, L., Pasini, A. F., Garbin, U., Davoli, A., Tosetti, M. L., Campagnola, M., Rigoni, A., Pastorino, A. M., Lo Cascio, V. & Sawamura, T. (2000). *J. Biol. Chem.* **275**, 12633–12638.
Cominacini, L., Rigoni, A., Pasini, A. F., Garbin, U., Davoli, A., Campagnola, M., Pastorino, A. M., Lo Cascio, V. & Sawamura, T. (2001). *J. Biol. Chem.* **276**, 13750–13755.
Drickamer, K. (1999). *Curr. Opin. Struct. Biol.* **9**, 585–590.
Drickamer, K. & Dodd, R. B. (1999). *Glycobiology*, **9**, 1357–1369.
Kataoka, H., Kume, N., Miyamoto, S., Minami, M., Morimoto, M., Hayashida, K., Hashimoto, N. & Kita, T. (2001). *Arterioscler. Thromb. Vasc. Biol.* **21**, 955–960.
Kataoka, H., Kume, N., Miyamoto, S., Minami, M., Moriwaki, H., Murase, T., Sawamura, T., Masaki, T., Hashimoto, N. & Kita, T. (1999). *Circulation*, **99**, 3110–3117.
Kita, T. (1999). *Circ. Res.* **84**, 1113–1115.
Kita, T., Kume, N., Minami, M., Hayashida, K., Murayama, T., Sano, H., Moriwaki, H., Kataoka, H., Nishi, E., Horiuchi, H., Arai, H. & Yokode, M. (2001). *Ann. NY Acad. Sci.* **947**, 199–205.
Li, D. & Mehta, J. L. (2000*a*). *Circulation*, **101**, 2889–2895.
Li, D. & Mehta, J. L. (2000*b*). *Arterioscler. Thromb. Vasc. Biol.* **20**, 1116–1122.
Li, H., Natarajan, K., Malchiodi, E. L., Margulies, D. H. & Mariuzza, R. A. (1998). *J. Mol. Biol.* **283**, 179–191.
Natarajan, K., Dimasi, N., Wang, J., Mariuzza, R. A. & Margulies, D. H. (2002). *Annu. Rev. Immunol.* **20**, 853–885.
Natarajan, K., Sawicki, M. W., Margulies, D. H. & Mariuzza, R. A. (2000). *Biochemistry*, **39**, 14779–14786.
Otwinowski, Z. & Minor, W. (1997). *Methods Enzymol.* **276**, 307–326.
Pflugrath, J. W. (1999). *Acta Cryst.* D**55**, 1718–1725.
Sawamura, T., Kume, N., Aoyama, T., Moriwaki, H., Hoshikawa, H., Aiba, Y., Tanaka, T., Miwa, S., Katsura, Y., Kita, T. & Masaki, T. (1997). *Nature (London)*, **386**, 73–77.
Sheriff, S., Chang, C. Y. & Ezekowitz, R. A. (1994). *Nature Struct. Biol.* **1**, 789–794.
Shi, X., Niimi, S., Ohtani, T. & Machida, S. (2001). *J. Cell Sci.* **114**, 1273–1282.
Weis, W. I. & Drickamer, K. (1994). *Structure*, **2**, 1227–1240.
Weis, W. I., Drickamer, K. & Hendrickson, W. A. (1992). *Nature (London)*, **360**, 127–134.
Weis, W. I., Kahn, R., Fourme, R., Drickamer, K. & Hendrickson, W. A. (1991). *Science*, **254**, 1608–1615.